# Delayed-feedback control of spatial bifurcations and chaos in open-flow models

Keiji Konishi,* Hideki Kokame, and Kentaro Hirata
*Department of Electrical and Electronic Systems, Osaka Prefecture University 1-1 Gakuen-cho, Sakai, Osaka 599-8531, Japan*
(Received 7 February 2000)

A delayed-feedback control scheme is presented for suppressing spatial bifurcation and chaotic behavior in open-flow models. It is shown that spatial bifurcation and chaotic behavior never occur when the delayed-feedback controller is designed such that the following two conditions are satisfied: all the poles of the transfer function of each site are inside a unit circle and the $H_\infty$ norm of the transfer function is less than 1. We provide a simple systematic procedure for design of the delayed-feedback controller. It is confirmed that our theoretical results agree well with the numerical simulations.

PACS number(s): 05.45.Gg, 07.05.Dz, 47.27.Rc, 47.62.+q

## I. INTRODUCTION

Controlling chaos has been actively investigated in the field of nonlinear science [1]. Ott, Grebogi, and Yorke (OGY) proposed a method which stabilizes chaotic motions onto desired unstable periodic orbits (UPOs) [2]. The delayed-feedback control (DFC) method proposed by Pyragas [3] does not require a reference signal corresponding to the desired UPO. The DFC method has been widely used for several real systems [1], since it is a practical scheme for experimental situations. The stability of the DFC method for simple low-dimensional chaotic systems has been analyzed [4–7], and a discrete-time version of the method was examined [8–13]. In recent years, investigations of spatiotemporal chaotic behavior and its control have attracted much interest [14–18]. Konishi, Hirai, and Kokame [15] proposed a decentralized delayed-feedback control (DDFC) for a one-way open coupled map lattice [19–21]. They obtained a stability condition for the control system to be stable. In order to design robust local controllers for uncertain parameter information, they gave a simple procedure which does not depend on the system size; however, this procedure takes into account only the internal stability of each site, but not the noise propagation in the lattice sites.

The dynamics of spatially extended nonlinear systems consisting of coupled low-dimensional nonlinear maps has created considerable interest [22]. Coupled map lattices (CMLs) have been particularly investigated by many researchers, since they exhibit a wide variety of novel and complex spatiotemporal behaviors. The CMLs can be classified into several types according to the connections and boundary conditions. The one-way open CML is a typical open-flow model [19–21]. Spatial bifurcations in the CML were discovered [19], and have been studied in detail in numerical simulations [20,21]. Yamaguchi investigated the phenomenon of spatial bifurcations in the CML and derived the bifurcation conditions [23]. Very recently, the spatial bifurcation condition and its mechanism in open-flow models were clarified by the $H_\infty$-norm concept of transfer function [24]. Reference [24] showed that spatial bifurcation never occurs when the $H_\infty$ norm is less than 1.

From the practical point of view, spatial bifurcation and chaotic behavior in real open-flow systems, such as turbulent behavior in pipe flows, are undesirable because of complicated and unpredictable oscillations. Therefore, we notice that suppression of spatial bifurcation and chaotic behavior will be an important subject. The DDFC method can suppress chaotic behavior in the one-way open CML under a noiseless environment [15]. However, it has the following three disadvantages: (1) it is not suitable for suppression of chaotic behavior under a noisy environment, (2) it cannot suppress spatial bifurcation, and (3) it cannot stabilize a class of open-flow models due to the inherent weak point of the DFC [8–13]. The present paper modifies the DDFC method to overcome the above disadvantages. The DDFC method [15] uses *static* controllers which guarantee only the internal stability of each site; on the contrary, our modified method uses *dynamic* controllers in order that each site is internally stable and the $H_\infty$ norm of each site is less than 1. Furthermore, we give a systematic procedure for the design of dynamic controllers and show that the theoretical results agree well with numerical simulations.

## II. STABILITY OF ONE-WAY OPEN CML

Let us consider a one-way open CML

$$x_i(n+1)=(1-\varepsilon)f[x_i(n)]+\varepsilon f[x_{i-1}(n)] \quad (i=1,2,\ldots), \tag{1}$$

where $x_i(n)\in\mathbb{R}$ is the system state of the $i$th lattice site at time $n$, $\varepsilon\in[0,1)$ is the coupling strength, and $f:\mathbb{R}\to\mathbb{R}$ is the local nonlinear map. We assume that the upper boundary $x_0(n)$ is fixed at $x_0(n)=x_f$, where $x_f$ is the fixed point of the local map $f$, that is, $x_f=f[x_f]$. The steady state of the CML is

$$[x_1(n) \quad x_2(n) \quad x_3(n) \quad \cdots]^T=[x_f \quad x_f \quad x_f \quad \cdots]^T. \tag{2}$$

Assume that the orbits at the upper sites [i.e., 1,2, . . . ,$(i-2)$th lattice sites] have already converged to the fixed point [i.e., $x_j(n)=x_f$ for $j=1,2,\ldots,(i-2)$]. If the $(i-1)$th and

*Author to whom correspondence should be addressed. FAX: +81-722-54-9907. Electronic address: konishi@ecs.ees.osakafu-u.ac.jp

 

$i$th lattice site states $x_{i-1}(n)$ and $x_i(n)$ are in the neighborhood of the fixed point $x_f$, the linearized dynamics of the $i$th lattice site is given as

$$y_i(n+1)=(1-\varepsilon)\Lambda y_i(n)+\varepsilon\Lambda y_{i-1}(n), \tag{3}$$

where

$$y_i(n):=x_i(n)-x_f, \quad y_{i-1}(n):=x_{i-1}(n)-x_f,$$

$$\Lambda:=\left.\frac{\partial f(x)}{\partial x}\right|_{x=x_f}.$$

The $\mathcal{Z}$ transforms [25] of $y_i(n+1)$, $y_i(n)$, and $y_{i-1}(n)$ are given, respectively, by

$$\mathcal{Z}[y_i(n+1)]=zY_i(z), \quad \mathcal{Z}[y_i(n)]=Y_i(z),$$

$$\mathcal{Z}[y_{i-1}(n)]=Y_{i-1}(z).$$

Taking the $\mathcal{Z}$ transforms of both sides of Eq. (3), we obtain

$$zY_i(z)=(1-\varepsilon)\Lambda Y_i(z)+\varepsilon\Lambda Y_{i-1}(z).$$

The relation of $Y_i(z)$ and $Y_{i-1}(z)$ is described as

$$Y_i(z)=G(z)Y_{i-1}(z), \tag{4}$$

where the transfer function $G(z)$ is

$$G(z)=\frac{\varepsilon\Lambda}{z-(1-\varepsilon)\Lambda}. \tag{5}$$

Let us recall the definitions of $H_\infty$ norm and of temporally spatially stability given in [24].

*Definition 1* [26]. Assume that a transfer function $F(z)$ has no poles outside of unit circle on complex plain. $H_\infty$ norm of the transfer function $F(z)$ is given by

$$\|F(z)\|_\infty:=\max_{\theta\in[0,2\pi]}|F(e^{j\theta})|.$$

*Definition 2* [24]. The spatiotemporal stability of steady state (2) in one-way open CML (1) is classified into the following three types:

(i) If $G(z)$ has a pole outside of the unit circle, it is temporally unstable (TU).

(ii) If $G(z)$ has a pole inside of the unit circle and the $H_\infty$ norm of $G(z)$ is less than 1 (i.e., $\|G(z)\|_\infty<1$), it is temporally spatially stable (TSS).

(iii) If $G(z)$ has a pole inside of the unit circle and the $H_\infty$ norm of $G(z)$ is greater than 1 (i.e., $\|G(z)\|_\infty>1$), it is temporally stable and spatially unstable (TSSU).

It is obvious that spatial bifurcation occurs in the one-way open CML only when steady state (2) is TSSU. This is because, if steady state (2) is TSSU, a tiny external noise in real systems or round-off error on computers at the upper sites significantly disturbs the lower sites. Hence the lower lattice site states $x_i(n)$ cannot keep staying on $x_f$. Furthermore, we can observe chaotic behaviors in the CML when steady state (2) is TU. The main purpose of this paper is to provide a control scheme which changes the stability of steady state (2) from TSSU/TU to TSS.

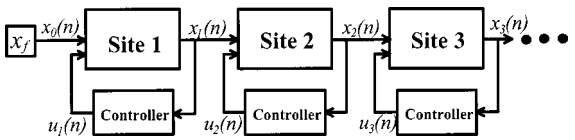


FIG. 1. One-way open CML with the decentralized controllers.

## III. STABILIZATION OF THE STEADY STATE

We notice that spatial bifurcation and chaotic behavior are observed in the one-way open CML when steady state (2) is TSSU or TU.

In order to suppress spatial bifurcation and chaotic behavior, we add a control term $u_i(n)$ to the right-hand side of Eq. (1):

$$x_i(n+1)=(1-\varepsilon)f[x_i(n)]+\varepsilon f[x_{i-1}(n)]+u_i(n)$$

$$(i=1,2,\ldots). \tag{6}$$

The control signal $u_i(n)$ is given by

$$w_i(n+1)=k_a w_i(n)+k_b[x_i(n)-x_i(n-1)],$$

$$u_i(n)=k_c w_i(n)+k_d[x_i(n)-x_i(n-1)], \tag{7}$$

where $k_a,k_b,k_c,k_d\in\mathbb{R}$ are the feedback gains. Since the variable $w_i(n)\in\mathbb{R}$ is the internal state variable of the $i$th controller at time $n$, it does not represent any physical values. In the field of control theory, most of the controllers usually employ such a variable to extend the dynamics of the controllers. We remark that controller (7) never changes the location of steady state (2). Figure 1 illustrates the one-way open CML with controller (7). This paper employs a *dynamic* delayed-feedback controller (7) instead of a *static* controller (i.e., $k_a=k_b=k_c=0$) used in [15]. Controller (7) can be regarded as a decentralized dynamic delayed-feedback controller proposed in [27,28]. The resulting closed-loop system consisting of system (6) and controller (7) can be linearized as

$$\begin{bmatrix} y_i(n+1) \\ y_i(n) \\ w_i(n+1) \end{bmatrix} = \begin{bmatrix} (1-\varepsilon)\Lambda+k_d & -k_d & k_c \\ 1 & 0 & 0 \\ k_b & -k_b & k_a \end{bmatrix} \begin{bmatrix} y_i(n) \\ y_i(n-1) \\ w_i(n) \end{bmatrix} + \begin{bmatrix} \varepsilon\Lambda \\ 0 \\ 0 \end{bmatrix} y_{i-1}(n). \tag{8}$$

The relation between $Y_i(z):=\mathcal{Z}[y_i(n)]$ and $Y_{i-1}(z):=\mathcal{Z}[y_{i-1}(n)]$ of system (8) is

$$Y_i(z)=\overline{G}(z)Y_{i-1}(z). \tag{9}$$

The transfer function $\overline{G}(z)$ is given as

$$\overline{G}(z)=\frac{N(z)}{D(z)},$$

where

$$N(z)=z(z-k_a)\varepsilon\Lambda,$$

$$D(z)=z^3-\{(1-\varepsilon)\Lambda+k_a+k_d\}z^2+\{k_d+k_ak_d-k_bk_c+k_a(1-\varepsilon)\Lambda\}z+k_bk_c-k_ak_d.$$

We notice that relation (9) corresponds to Eq. (4). Since the difference between Eqs. (9) and (4) is only the degree of the transfer functions $G(z)$ and $\bar{G}(z)$, definition 2 can be extended to the controlled CML consisting Eqs. (6) and (7).

*Definition 3*. The spatiotemporal stability of steady state (2) in the CML controlled by Eqs. (7) is classified into the following three types.

(i) If $\bar{G}(z)$ has at least one pole outside of the unit circle, it is TU.

(ii) If all the poles of $\bar{G}(z)$ are inside of the unit circle and $\|\bar{G}(z)\|_\infty<1$, it is TSS.

(iii) If all the poles of $\bar{G}(z)$ are inside of the unit circle and $\|\bar{G}(z)\|_\infty>1$, it is TSSU.

In general, it is not easy to determine the feedback gains such that steady state (2) becomes TSS. This paper shall provide a simple systematic procedure how to determine the feedback gains for suppression of spatial bifurcation and for stabilization of chaotic behavior. If we choose the feedback gains as

$$k_a=k_b=\frac{(1-\varepsilon)\Lambda}{(1-\varepsilon)\Lambda-1},\quad k_c=k_d=-\frac{(1-\varepsilon)^2\Lambda^2}{(1-\varepsilon)\Lambda-1},\tag{10}$$

then the transfer function $\bar{G}(z)$ can be reduced to

$$\bar{G}(z)=\frac{\varepsilon\Lambda z(z-k_a)}{z^3}.\tag{11}$$

The closed-loop system consisting of Eqs. (6) and (7) shows deadbeat behavior, since all the poles of $\bar{G}(z)$ are zero. The $H_\infty$ norm of $\bar{G}(z)$ is

$$\|\bar{G}(z)\|_\infty=\max_{\theta\in[0,2\pi]}\left|\frac{\varepsilon\Lambda e^{j\theta}(e^{j\theta}-k_a)}{e^{j3\theta}}\right|$$

$$=|\varepsilon\Lambda|\max_{\theta\in[0,2\pi]}|e^{j\theta}-k_a|$$

$$=|\varepsilon\Lambda|\max_{\theta\in[0,2\pi]}\sqrt{k_a^2-2k_a\cos\theta+1}.$$

Hence, the $H_\infty$ norm of $\bar{G}(z)$ can be given by

$$\|\bar{G}(z)\|_\infty=\begin{cases}|\varepsilon\Lambda(1+k_a)| & \text{if } k_a\geqslant 0,\\ |\varepsilon\Lambda(1-k_a)| & \text{if } k_a\leqslant 0.\end{cases}$$

Spatial bifurcation and chaotic behavior do not occur in the CML only when $\|\bar{G}(z)\|_\infty<1$. From the above results, we can provide a systematic procedure for design of the feedback gains

(1) The information $(\Lambda,\varepsilon)$ is known and the gain $k_a$ is estimated from Eq. (10).

(2) If $k_a\geqslant 0$, then go to step (3); if $k_a\leqslant 0$, then go to step (4).

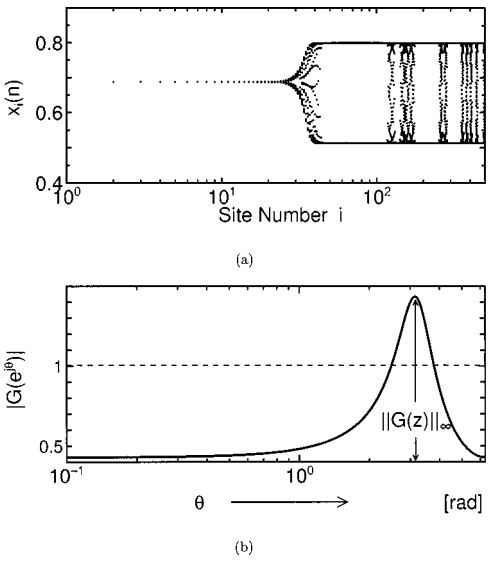


FIG. 2. Spatial bifurcation and gain diagrams without control. The parameters are fixed at $a=3.2$, $\varepsilon=0.55$. (a) Spatial bifurcation diagram. (b) Gain diagram of $G(z)$.

(3) If $|\varepsilon\Lambda(1+k_a)|<1$, then go to step (5): otherwise, stop.

(4) If $|\varepsilon\Lambda(1-k_a)|<1$, then go to step (5): otherwise, stop.

(5) The feedback gains are chosen as Eqs. (10).

After step (5), the steady state of the controlled CML becomes TSS. It should be noted that even if we cannot reach step (5), the steady state may become TSS by gains other than Eqs. (10).

## IV. NUMERICAL EXAMPLES

### A. Suppression of spatial bifurcation

We use the logistic map $f(x)=ax(1-x)$ as the local nonlinear map. The fixed point is described as $x_f=(a-1)/a$; thus, we obtain $\Lambda=2-a$. The system parameter and coupling strength are fixed at $(a,\varepsilon)=(3.2,0.55)$. The system size is $N=50$. Figure 2(a) shows the spatial bifurcation diagram without control. In order to neglect the transient behavior, $x_i(n)$ is plotted for $n=49\,980, 49\,981, \ldots, 50\,000$. Initial conditions are $x_i(0)=x_f$ for $i=1,2,\ldots,500$. A tiny random noise is added to the upper boundary site: $x_0(n)=x_f+10^{-5}\eta_n$, where $\eta_n\in[-1,+1]$ is the uniform random value. As one can see, we can observe spatial bifurcation in the CML. The gain diagram of the transfer function $G(z)$ is shown in Fig. 2(b). It can be seen that the maximum gain—that is, $\|G(z)\|_\infty$—is greater than 1, and the pole of $G(z)$ [i.e., $z=(1-\varepsilon)\Lambda$] is inside of the unit circle. Since steady state (2) is TSSU, we can see the spatial bifurcation as shown in Fig. 2(a).

Now we shall suppress the spatial bifurcation using dynamic delayed-feedback control (7). It is undesirable for the control signal to be large, since a large signal may make the control system fall into a divergence regime. In order to avoid the divergence, we employ a local watcher for every site [15]. Each local watcher is described as

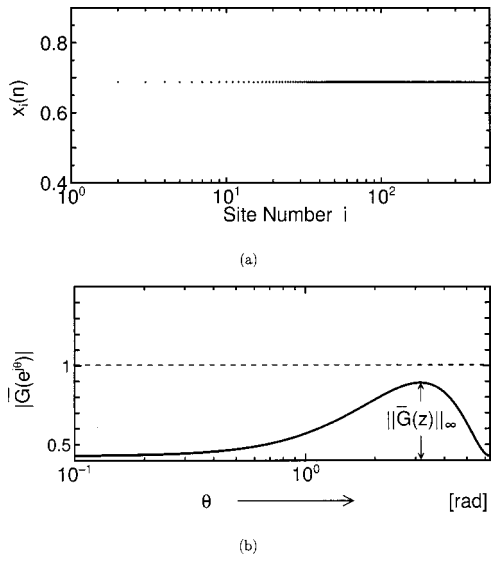


FIG. 3. Spatial bifurcation and gain diagrams with control. The parameters are the same as in Fig. 2. (a) Spatial bifurcation diagram. (b) Gain diagram of $\bar{G}(z)$.

$$u_i(n)=\begin{cases} u_i(n) & \text{if } |u_i(n)|\leqslant \nu, \\ 0 & \text{if } |u_i(n)|>\nu, \end{cases}$$

where the threshold $\nu$ is a small positive value. The parameters and the noise are the same as Fig. 2. The feedback gains are chosen by our systematic procedure (i.e., $k_a=k_b=0.350\,65$, $k_c=k_d=-0.189\,35$). The watcher threshold is set as $\nu=0.01$. Figure 3(a) shows the spatial bifurcation diagram with control. The control starts at time $n=10\,000$. We cannot see spatial bifurcation in the CML. The gain diagram of the transfer function of the closed-loop system $\bar{G}(z)$ is shown in Fig. 3(b). Since $\|\bar{G}(z)\|_\infty$ is less than 1 and the poles of $\bar{G}(z)$ are inside the unit circle, the steady state is TSS. Figure 4 shows the spatiotemporal behavior of the controlled CML. The parameters, noise, and gains are the same as Fig. 3. The control starts at time $n=200$. We can observe that site states $x_i(n)$ converge on $x_f$ in the order of the site number $i$.

### B. Stabilizing chaotic behavior

Let us consider two numerical examples. First of all, we use a logistic map as the local nonlinear map. The system

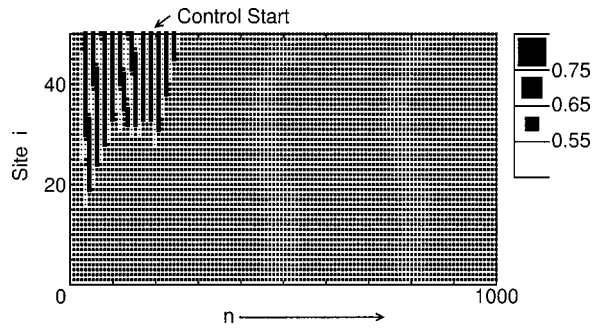


FIG. 4. Space-time plot of the controlled one-way open CML with logistic maps. The parameters, noise, and gains are the same as in Fig. 3.

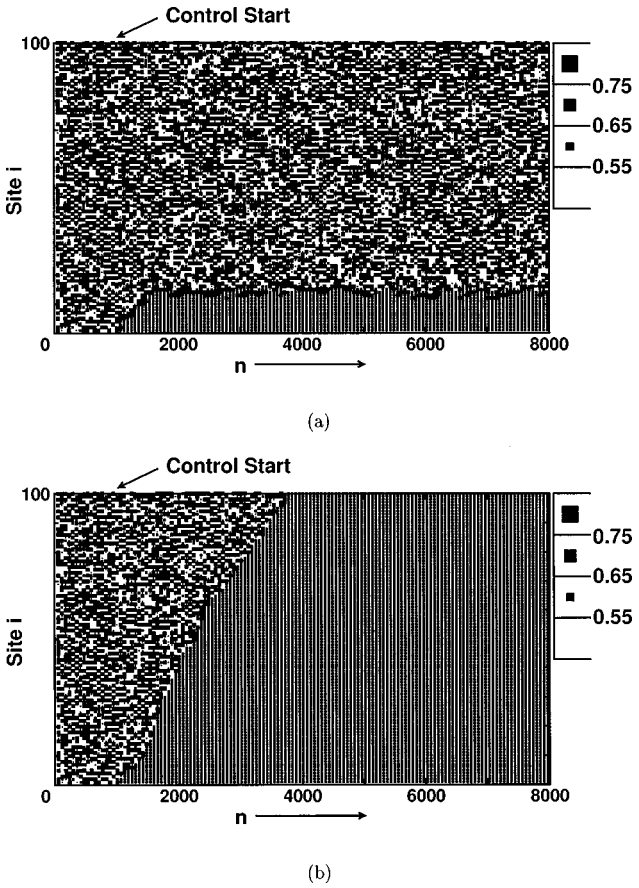


FIG. 5. Space-time plots of the one-way open coupled logistic map lattice controlled by (a) static controller ($k_a=k_b=k_c=0$, $k_d=0.9$) and (b) dynamic controller ($k_a=k_b=0.6322$, $k_c=k_d=1.0868$). The parameters are set as $a=3.91$, $\varepsilon=0.1$, and $\nu=0.05$.

parameter and coupling strength are fixed at $(a,\varepsilon)=(3.91,0.1)$. The system size is $N=100$. The fixed point is $x_f=0.7442$. From definition 2, we notice that steady state (2) is TU. The initial conditions and the tiny random noise are the same as Fig. 3. Spatiotemporal chaotic behavior occurs in the CML without control. Now we shall try to stabilize the chaotic behavior by the following controllers: the static delayed-feedback controller proposed in [15] [i.e., controller (7) with $k_a=k_b=k_c=0$] and dynamic delayed-feedback controller (7). The static controller is set as $k_a=k_b=k_c=0$ and $k_d=0.9$, which satisfies the stability condition in [15]. On the other hand, the feedback gains of dynamic controller (7) are chosen by our systematic procedure in Sec. III (i.e., $k_a=k_b=0.6322$, $k_c=k_d=1.0868$). The watcher threshold is set as $\nu=0.05$. Figure 5(a) shows the spatiotemporal behavior of the CML controlled by the static controller. The control starts at time $n=1000$. The upper sites states $x_i(n)$ converge on $x_f$; however, the lower sites behave chaotically. This is because the stability analysis in [15] does not consider noise propagation. Figure 5(b) is the spatiotemporal behavior of the CML controlled by dynamic controller (7). It can be seen that all sites converge on the fixed point $x_f$ in the order of the site number $i$. The reason for our successful stabilization is that the feedback gains $(k_a,k_b,k_c,k_d)$ of dynamic controller (7) are designed such that the $H_\infty$ norm of $\bar{G}(z)$ is less than

1. In other words, they are designed in consideration of the noise propagation in the lattice sites.

For the second example, we use a piecewise linear map $f(x)=a(x+1)$ if $x\leqslant -0.5$, $ax$ if $|x|\leqslant 0.5$, and $a(x-1)$ if $0.5\leqslant x$, where $a$ is the system parameter. The fixed point is $x_f=0$; thus, we obtain $\Lambda=a$. The system parameter and coupling strength are fixed at $(a,\varepsilon)=(2.5,0.1)$. The system size is $N=100$. Since $\Lambda$ is greater than 1, we notice that the original DDFC (i.e., static delayed-feedback control) never stabilizes steady state (2) due to the inherent weak point of the DFC (see Fig. 1 in [15]). On the contrary, for $\Lambda=2.5$ and $\varepsilon=0.1$, we can reach step (5) in our controller-design procedure. This implies that the controller designed our procedure can stabilize steady state (2). Figure 6 shows the space-time diagram of the controlled coupled piecewise linear map lattice. The control starts at time $n=1000$. It can be seen that all the sites converge to the fixed point $x_f=0.0$ successfully.

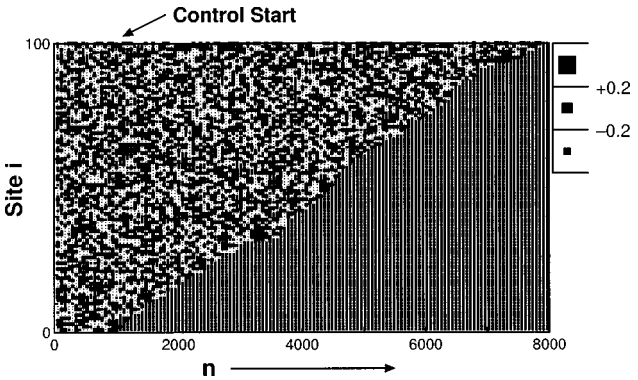


FIG. 6. Space-time plots of the one-way open coupled piecewise-linear map lattice controlled by dynamic controller ($k_a=k_b=1.8$, $k_c=k_d=-4.05$). The parameters are set as $a=2.5$, $\varepsilon=0.1$, and $\nu=0.09$.

## V. CONCLUSIONS

We have shown that the dynamic version of the DDFC method is a useful scheme for suppressing spatial bifurcation and chaotic behavior in open-flow models. The main results obtained in this paper are shown below: Spatial bifurcation and chaotic behavior never occur when the delayed-feedback controller is designed such that the poles of $\overline{G}(z)$ are all located in the unit circle and $\|\overline{G}(z)\|_\infty$ is less than 1. We provide a simple systematic procedure for the design of the delayed-feedback controller. Our theoretical results agree well with the numerical simulations for the coupled logistic and piecewise-linear maps. We plan in the near future to realize our control system on electronic circuits and to show experimental evidence of our system.

[1] G. Chen and X. Dong, *From Chaos to Order* (World Scientific, Singapore, 1998).
[2] E. Ott, C. Grebogi, and J. A. Yorke, Phys. Rev. Lett. **64**, 1196 (1990).
[3] K. Pyragas, Phys. Lett. A **170**, 421 (1992).
[4] M. E. Bleich and J. E. S. Socolar, Phys. Lett. A **210**, 87 (1996).
[5] W. Just, T. Bernard, M. Ostheimer, E. Reibold, and H. Benner, Phys. Rev. Lett. **78**, 203 (1997).
[6] H. Nakajima, Phys. Lett. A **232**, 207 (1997).
[7] H. Kokame and T. Mori (unpublished).
[8] S. Bielawski, D. Derozier, and P. Glorieux, Phys. Rev. A **47**, R2492 (1993).
[9] T. Ushio, IEEE Trans. Circuits and Syst. I: Fundam. Theory Appl. **43**, 815 (1996).
[10] M. de Sousa Vieira and A. J. Lichtenberg, Phys. Rev. E **54**, 1200 (1996).
[11] M. Ishii, K. Konishi, and H. Kokame, Phys. Lett. A **235**, 603 (1997).
[12] K. Konishi, M. Ishii, and H. Kokame, Phys. Rev. E **54**, 3455 (1996).
[13] K. Konishi, M. Ishii, and H. Kokame, IEEE Trans. Circuits Syst., I: Fundam. Theory Appl. **46**, 1285 (1999).
[14] G. Hu, Z. Qu, and K. He, Int. J. Bifurcation Chaos Appl. Sci. Eng. **5**, 901 (1997).
[15] K. Konishi, M. Hirai, and H. Kokame, Phys. Rev. E **58**, 3055 (1998).
[16] K. Konishi and H. Kokame, Physica D **100**, 423 (1997).
[17] K. Konishi and H. Kokame, Physica D **127**, 1 (1999).
[18] K. Konishi, H. Kokame, and K. Hirata, IEEE Trans. Circuits Fundam. Theory Appl. Syst., I:, Fundam. Theory Appl. (to be published).
[19] K. Kaneko, Phys. Lett. **111A**, 321 (1985).
[20] F. H. Willeboordse and K. Kaneko, Phys. Rev. Lett. **73**, 533 (1994).
[21] F. H. Willeboordse and K. Kaneko, Physica D **86**, 428 (1995).
[22] K. Kaneko, Chaos **2**, 279 (1992).
[23] A. Yamaguchi, Int. J. Bifurcation Chaos Appl. Sci. Eng. **7**, 1529 (1997).
[24] K. Konishi, H. Kokame, and K. Hirata, Phys. Lett. A **263**, 307 (1999).
[25] K. Ogata, *Discrete-Time Control System*, 2nd ed. (Prentice-Hall, Englewood Cliffs, NJ, 1995).
[26] A. A. Stoorvogel, A. Saberi, and B. M. Chen, Int. J. Robust Nonlinear Control **4**, 457 (1994).
[27] K. Konishi and H. Kokame, Phys. Lett. A **248**, 359 (1999).
[28] S. Yamamoto and T. Ushio (unpublished).